

Association of White Matter Hyperintensity Markers on MRI and Long-term Risk of Mortality and Ischemic Stroke

The SMART-MR Study

Rashid Ghaznawi, MD, MSc, Mirjam I. Geerlings, PhD, Myriam Jaarsma-Coes, MSc, Jeroen Hendrikse, MD, PhD, and Jeroen de Bresser, MD, PhD, on behalf of the UCC-Smart Study Group

Neurology® 2021;96:e2172-e2183. doi:10.1212/WNL.00000000000011827

Correspondence

Dr. Geerlings
m.geerlings@umcutrecht.nl

Abstract

Objective

To determine whether white matter hyperintensity (WMH) markers on MRI are associated with long-term risk of mortality and ischemic stroke.

Methods

We included consecutive patients with manifest arterial disease enrolled in the Second Manifestations of Arterial Disease–Magnetic Resonance (SMART-MR) study. We obtained WMH markers (volume, type, and shape) from brain MRI scans performed at baseline using an automated algorithm. During follow-up, occurrence of death and ischemic stroke was recorded. Using Cox regression, we investigated associations of WMH markers with risk of mortality and ischemic stroke, adjusting for demographics, cardiovascular risk factors, and cerebrovascular disease.

Results

We included 999 patients (59 ± 10 years; 79% male) with a median follow-up of 12.5 years (range 0.2–16.0 years). A greater periventricular or confluent WMH volume was independently associated with a greater risk of vascular death (hazard ratio [HR] 1.29, 95% confidence interval [CI] 1.13–1.47) for a 1-unit increase in natural log-transformed WMH volume and ischemic stroke (HR 1.53, 95% CI 1.26–1.86). A confluent WMH type was independently associated with a greater risk of vascular (HR 1.89, 95% CI 1.15–3.11) and nonvascular death (HR 1.65, 95% CI 1.01–2.73) and ischemic stroke (HR 2.83, 95% CI 1.36–5.87). A more irregular shape of periventricular or confluent WMH, as expressed by an increase in concavity index, was independently associated with a greater risk of vascular (HR 1.20, 95% CI 1.05–1.38 per SD increase) and nonvascular death (HR 1.21, 95% CI 1.03–1.42) and ischemic stroke (HR 1.28, 95% CI 1.05–1.55).

Conclusions

WMH volume, type, and shape are associated with long-term risk of mortality and ischemic stroke in patients with manifest arterial disease.

RELATED ARTICLE

Editorial

White Matter
Hyperintensities: How
Much (and What Shape) Is
Too Much?

Page 781

From the Department of Radiology (R.G., J.H.) and Julius Center for Health Sciences and Primary Care (R.G., M.I.G.), University Medical Center Utrecht and Utrecht University; and Department of Radiology (M.J.-C., J.d.B.), Leiden University Medical Center, the Netherlands.

Go to [Neurology.org/N](https://www.neurology.org/N) for full disclosures. Funding information and disclosures deemed relevant by the authors, if any, are provided at the end of the article.

The Article Processing Charge was funded by European Research Council.

The Utrecht Cardiovascular Cohort-Second Manifestations of Arterial Disease Study Group is listed in Appendix 2.

This is an open access article distributed under the terms of the Creative Commons Attribution-NonCommercial-NoDerivatives License 4.0 (CC BY-NC-ND), which permits downloading and sharing the work provided it is properly cited. The work cannot be changed in any way or used commercially without permission from the journal.

Glossary

CI = confidence interval; CSVD = cerebral small vessel disease; FLAIR = fluid-attenuated inversion recovery; HR = hazard ratio; SMART-MR = Second Manifestations of Arterial Disease–Magnetic Resonance; TE = echo time; TI = inversion time; TR = repetition time; WMH = white matter hyperintensities.

White matter hyperintensities (WMH) of presumed vascular origin are frequently observed in older individuals on brain MRI and are an important cause of cognitive decline and dementia.¹⁻³ They are considered hallmark features of cerebral small vessel disease (CSVD).^{4,5}

WMH are heterogeneous lesions that correspond to different underlying brain parenchymal changes.⁶⁻⁸ Previous studies on CSVD mainly focused on WMH volume as a marker for CSVD severity.^{4,9-12} However, there is evidence to suggest that other markers of WMH may also provide clinically relevant information on severity and prognosis of CSVD.^{6,7,13-16} Specifically, histopathologic studies reported that smooth and periventricular WMH are associated with mild changes of the brain parenchyma, whereas irregular and confluent WMH are associated with more severe parenchymal changes, including loss of myelin and incomplete parenchymal destruction.^{6,13} We previously developed an automated MRI method to assess in vivo advanced WMH markers (volume, type, and shape).¹⁴ Using this algorithm, we reported differences in advanced WMH markers such as shape in frail elderly patients, patients with diabetes mellitus, and patients with lacunes on MRI.¹⁴⁻¹⁶ These findings suggest that advanced WMH MRI markers may provide clinically important information on CSVD severity.

The relationship between advanced WMH markers and long-term clinical outcomes, however, is not clear. Examining this relationship is of importance as WMH markers may aid in future patient selection for preventive treatment to ameliorate the risk of CSVD-related death and ischemic stroke. Therefore, in the present study, we aimed to assess whether WMH volume, type, and shape were associated with greater risk of mortality (including vascular death) and ischemic stroke in patients with manifest arterial disease over 12 years of follow-up.

Methods

Standard Protocol Approvals, Registrations, and Patient Consents

The Second Manifestations of Arterial Disease–Magnetic Resonance (SMART-MR) study was approved by the medical ethics committee of the University Medical Center Utrecht according to the guidelines of the Declaration of Helsinki of 1975. Written informed consent was obtained from all patients participating in the SMART-MR study.

Study Population

We used data from the SMART-MR study.¹⁷ The SMART-MR study is a prospective cohort study at the University

Medical Center Utrecht with the aim of investigating risk factors and consequences of brain changes on MRI in patients with manifest arterial disease.¹⁷ A total of 1,309 middle-aged and older adult patients referred to our medical center for treatment of manifest arterial disease (cerebrovascular disease, manifest coronary artery disease, abdominal aortic aneurysm, or peripheral arterial disease) were included for baseline measurements between 2001 and 2005.¹⁷ During a 1-day visit to the University Medical Center Utrecht, ultrasonography of the carotid arteries to measure the intima-media thickness (mm), blood and urine samplings, a physical examination, neuropsychological assessment, and a 1.5T brain MRI scan were performed.¹⁷ We used questionnaires for the assessment of demographics, medical history, risk factors, medication use, and cognitive and physical functioning.¹⁷

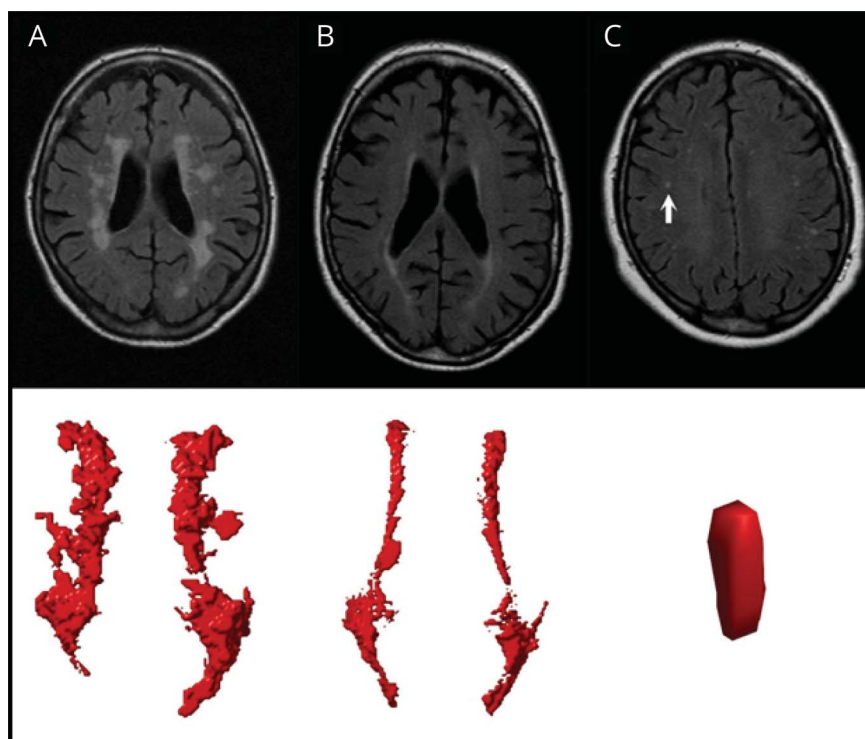
Vascular Risk Factors

We assessed age, sex, smoking habits, and alcohol intake at baseline using questionnaires. The body mass index (BMI) was calculated (kg/m^2) by measuring weight and height. We measured systolic blood pressure (mm Hg) and diastolic blood pressure (mm Hg) 3 times with a sphygmomanometer and the average of these measurements was calculated. Hypertension was defined as a mean systolic blood pressure of >160 mm Hg, a mean diastolic blood pressure of >95 mm Hg, or the self-reported use of antihypertensive drugs.¹⁷ To determine glucose and lipid levels, an overnight fasting venous blood sample was taken. We defined diabetes mellitus as a fasting serum glucose level of ≥ 7.0 mmol/L or use of glucose-lowering medication or a known history of diabetes.¹⁷ The degree of carotid artery stenosis at both sides was assessed with color Doppler-assisted duplex scanning using a 10 MHz linear-array transducer (ATL Ultramark 9).¹⁸ Blood flow velocity patterns were used to evaluate the severity of carotid artery stenosis and the greatest stenosis observed on the left or right side of the common or internal carotid artery was taken to determine the severity of carotid artery disease.¹⁸ We defined a carotid artery stenosis $\geq 70\%$ as a peak systolic velocity >210 cm/s.¹⁸

Brain MRI

MRI of the brain was performed on a 1.5T whole-body system (Gyrosan ACS-NT; Philips Medical Systems, Best, the Netherlands) using a standardized scan protocol.^{17,19} Transversal fluid-attenuated inversion recovery (FLAIR) (repetition time [TR] 6,000 ms; echo time [TE] 100 ms; inversion time [TI] 2,000 ms), T1-weighted (TR 235 ms; TE 2 ms), T1-weighted inversion recovery (TR 2,900 ms; TE 22 ms; TI 410 ms), and T2-weighted images (TR 2,200 ms; TE 11 ms) were acquired with a voxel size of $1.0 \times 1.0 \times 4.0$ mm³ and

Figure 1 White Matter Hyperintensities (WMH) on Fluid-Attenuated Inversion Recovery (FLAIR) Images With Corresponding Visualizations in the Automated Algorithm



Examples of confluent (A), periventricular (B), and deep (C) WMH on FLAIR images with the corresponding visualizations in our algorithm shown below. The deep WMH lesion (arrow) is reconstructed in the coronal view, while the periventricular and confluent WMH are viewed from a transverse perspective. Note that the coronal reconstruction of the deep WMH lesion (C) may be influenced by the slice thickness and the lesion may be more punctiform. The confluent WMH lesion in (A) showed a volume of 11.57 mL with an accompanying deep WMH volume of 0.25 mL. The periventricular WMH lesion in (B) showed a volume of 4.98 mL without any accompanying deep WMH lesions. The deep WMH lesion in (C) showed a volume of 0.02 mL with an accompanying periventricular and deep WMH volume of 2.12 and 0.49 mL, respectively.

contiguous slices.^{14,19} A neuroradiologist blinded to patient characteristics visually rated brain infarcts on the T1-weighted, T2-weighted, and FLAIR images of the MRI scans. We defined lacunes as focal lesions between 3 and 15 mm according to the STRIVE criteria.⁴ Nonlacunar lesions were categorized into large infarcts (i.e., cortical infarcts and subcortical infarcts not involving the cerebral cortex) and those located in the brainstem or cerebellum.¹⁴

WMH Volumes

WMH and brain volumes (intracranial volume and total brain volume) were obtained using the *k*-nearest neighbor (kNN) automated segmentation program on the T1-weighted, FLAIR, and T1-weighted inversion recovery sequences of the MRI scans.^{19,20} WMH segmentations were visually assessed by an investigator (R.G.) using an image processing framework (MeVisLab 2.7.1.; MeVis Medical Solutions AG, Bremen, Germany) to ensure that cerebral infarcts were correctly removed from the WMH segmentations.¹⁴ Next, we performed ventricle segmentation using the fully automated lateral ventricle delineation (ALVIN) algorithm in Statistical Parametric Mapping 8 (SPM8, Wellcome Trust Centre for Neuroimaging, University College London, UK) for MATLAB (The MathWorks, Inc., Natick, MA).¹⁴ The procedure is described in detail elsewhere.^{14,21} We labeled WMH according to their continuity with the margins of the lateral ventricle and their extension from the lateral ventricle into the white matter.¹⁴ Periventricular WMH were defined as lesions contiguous with the margins of the lateral ventricles and

extending up to 10 mm from the lateral ventricle into the white matter.¹⁴ We defined confluent WMH as lesions contiguous with the margins of the lateral ventricles and extending more than 10 mm from the lateral ventricles into the white matter.¹⁴ We defined deep WMH as lesions that were separated from the margins of the lateral ventricles.¹⁴ Examples of periventricular, confluent, and deep WMH visualized in our algorithm are shown in figure 1. Total WMH volume was calculated as the sum of deep WMH and periventricular or confluent WMH.

WMH Types

We categorized patients into the following 3 WMH types: periventricular WMH type without deep WMH, periventricular WMH type with deep WMH, and a confluent WMH type. We did not categorize the latter type according to presence or absence of deep WMH as the number of patients with a confluent WMH without deep WMH ($n = 5$) was insufficient to perform statistical analyses.¹⁴

WMH Shape Markers

We hypothesized that a more irregular shape of WMH may indicate more severe cerebral parenchymal damage based on previous histopathologic studies.^{6-8,13,22,23} The degree to which deep WMH are punctiform or ellipsoidal may also provide information on CSVD severity.¹⁵

Irregularity of periventricular or confluent WMH was quantified using the concavity index and fractal dimension. In

Table 1 Baseline Characteristics of the Study Sample (n = 999)

Characteristics	Values
Age, y	59 ± 10
Sex, % men	79.0
BMI, kg/m ²	27 ± 4
Smoking, pack-years ^a	18 (0, 50)
Alcohol intake, % current	74
Hypertension, %	51
Diabetes mellitus, %	20
Infarcts on MRI, %	
Large	12
Cerebellar	4
Brainstem	2
Lacunae	19
WMH volumes, mL ^a	
Total	0.9 (0.2, 6.4)
Periventricular or confluent	0.7 (0.1, 5.3)
Deep	0.1 (0.0, 0.8)
WMH types, %	
Periventricular	78
With deep	42
Without deep	36
Confluent	22
WMH shape markers	
Periventricular or confluent	
Concavity index	1.06 ± 0.11
Fractal dimension	1.24 ± 0.22
Deep	
Eccentricity	0.48 ± 0.14
Fractal dimension	1.45 ± 0.15

Abbreviations: BMI = body mass index; WMH = white matter hyperintensities. Characteristics are presented as mean ± SD or %.

^a Median (10th percentile, 90th percentile).

previous work, we established that the concavity index was a robust shape marker that showed a normal distribution in the study sample and provided information on WMH shape irregularity based on volume and surface area.^{14,24} The concavity index was calculated by reconstructing convex hulls and calculating volume and surface area ratios of lesions, in which a higher concavity index value corresponds to a more irregular shape of periventricular or confluent WMH.¹⁴ Fractal dimension was calculated using the box counting method and was used to quantify irregularity of periventricular or

confluent WMH and of deep WMH.^{14,25,26} A higher fractal dimension value indicated a more irregular WMH shape. As patients frequently show multiple deep WMH, a mean value for the fractal dimension was calculated across all deep WMH per patient.

The degree to which deep WMH are punctiform or ellipsoidal was assessed using the eccentricity, which was calculated by dividing the minor axis of a deep WMH lesion by its major axis.^{14,15} A high eccentricity value corresponded to a

Table 2 Results of Cox Proportional Hazard Regression Analyses With Total, Periventricular or Confluent, and Deep White Matter Hyperintensity (WMH) Volumes (All Natural Log-Transformed) as Independent Variables and All-Cause, Vascular-Related, and Nonvascular-Related Death and Ischemic Stroke as Dependent Variables

	Deaths or events, n	N per 1,000 person-years	Model 1, estimate (95% CI)	Model 2, estimate (95% CI)
Total WMH				
All-cause death	274	24.2	1.32 (1.19–1.46)	1.22 (1.10–1.36)
Vascular death	149	13.2	1.47 (1.29–1.68)	1.32 (1.14–1.51)
Nonvascular death	125	11.1	1.15 (0.99–1.34)	1.11 (0.95–1.30)
Ischemic stroke	75	6.8	1.79 (1.48–2.16)	1.58 (1.29–1.93)
Periventricular or confluent WMH				
All-cause death	274	24.2	1.29 (1.17–1.42)	1.20 (1.09–1.33)
Vascular death	149	13.2	1.43 (1.26–1.63)	1.29 (1.13–1.47)
Nonvascular death	125	11.1	1.14 (0.99–1.32)	1.10 (0.95–1.28)
Ischemic stroke	75	6.8	1.73 (1.45–2.08)	1.53 (1.26–1.86)
Deep WMH				
All-cause death	212	30.8	1.13 (1.04–1.24)	1.10 (1.01–1.21)
Vascular death	122	17.8	1.15 (1.03–1.30)	1.11 (0.98–1.25)
Nonvascular death	90	13.1	1.10 (0.96–1.26)	1.10 (0.96–1.26)
Ischemic stroke	62	9.4	1.24 (1.05–1.46)	1.18 (0.99–1.40)

Abbreviation: CI = confidence interval.

Estimates represent hazard ratios (95% CI) for a 1 unit increase in natural log-transformed WMH volumes. Model 1: adjusted for age, sex, and intracranial volume. Model 2: model 1 in addition adjusted for large infarcts on MRI, lacunes on MRI, diastolic blood pressure, systolic blood pressure, diabetes mellitus, body mass index, and smoking pack-years at baseline.

punctiform deep WMH lesion, whereas a low value corresponded to an ellipsoidal lesion.^{27,28} A mean value for the eccentricity was calculated across all deep WMH per patient.

Clinical Outcomes

Patients received a questionnaire every 6 months to provide information on outpatient clinic visits and hospitalization.¹⁸ If a fatal or nonfatal event was reported, original source documents were obtained and reviewed to determine the cause of the event. All possible events were audited independently by 3 physicians of the end point committee.¹⁸ Follow-up of patients was performed until death, refusal of further participation, or loss to follow-up. Vascular-related death was defined as death caused by myocardial infarction, stroke, sudden death (unexpected cardiac death occurring within 1 hour after onset of symptoms, or within 24 hours given convincing circumstantial evidence), congestive heart failure, or rupture of an abdominal aortic aneurysm.¹⁸ We defined nonvascular-related death as death caused by cancer, infection, unnatural death, or death from another nonvascular cause.¹⁸ Ischemic stroke was defined as the occurrence of relevant clinical features that caused an increase in impairment of at least 1 grade on the modified Rankin Scale, with or without a new relevant ischemic lesion on brain imaging.¹⁸

Study Sample

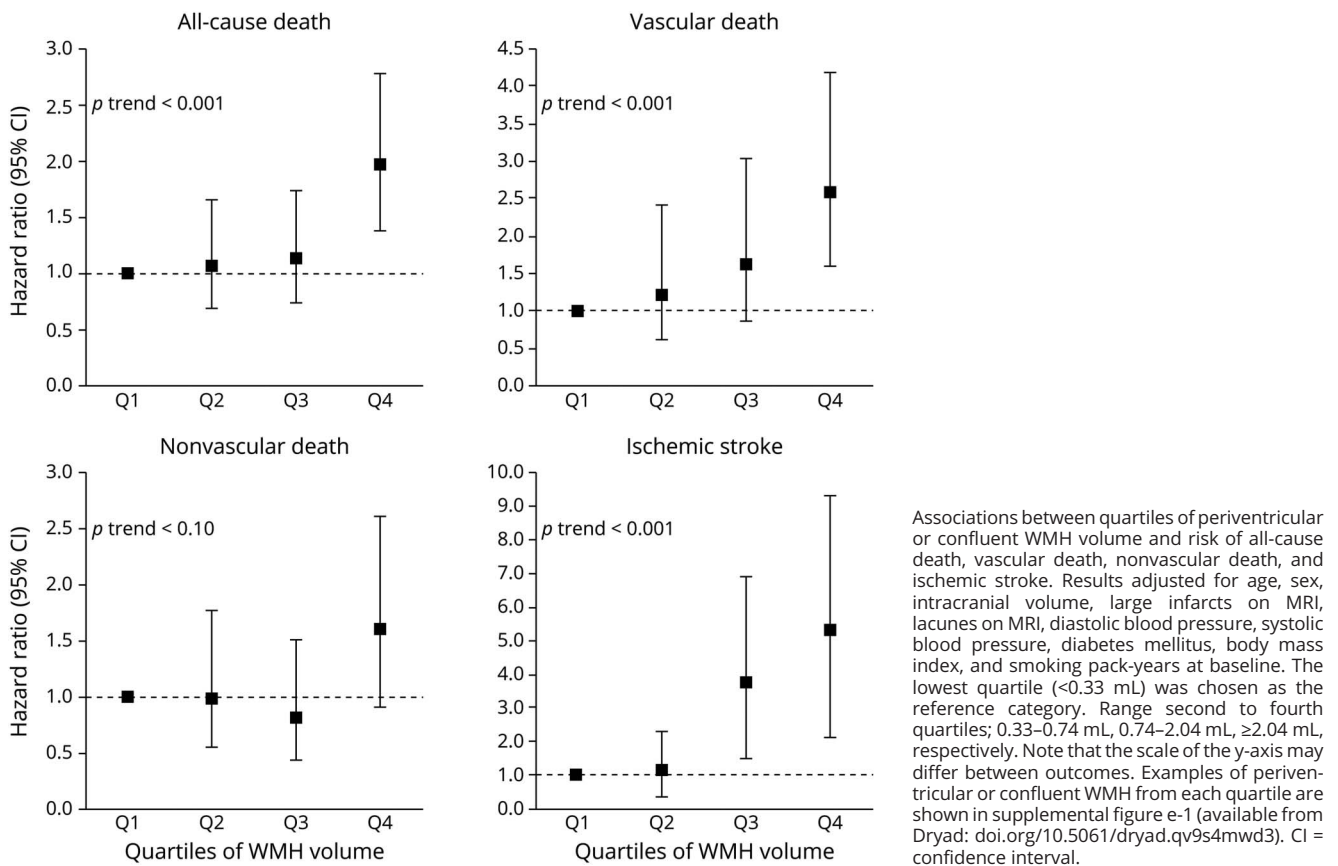
Of the 1,309 patients included, MRI data were irretrievable for 19 patients and 239 patients had missing data of one or more MRI sequences due to logistic reasons or motion artifacts. Forty-four of the remaining 1,051 patients had unreliable brain volume data due to motion artifacts in all 3 MRI sequences. Four patients were excluded due to undersegmentation of WMH by the automated segmentation algorithm and another 4 patients were excluded because they did not have any WMH greater than 5 voxels. As a result, 999 patients were included in the current study.

Statistical Analysis

Baseline characteristics of the study sample were reported as means or percentages where applicable.

Patients were followed from the date of the MRI until ischemic stroke, death, loss to follow-up, or end of follow-up (March 2017), whichever came first. Cox proportional hazard analysis was used to estimate hazard ratios (HRs) for the occurrence of all-cause, vascular-related, and nonvascular-related death and ischemic stroke associated with WMH volumes, type, and shape markers. The proportional hazards assumption was checked by inspection of Schoenfeld

Figure 2 Risk of Mortality and Ischemic Stroke in Relation to Quartiles of Periventricular or Confluent White Matter Hyperintensity (WMH) Volume at Baseline



residuals. We concluded that the proportional hazards assumption was met for all covariates.

To reduce the risk of bias due to complete case analysis, we performed chained equations imputation on missing covariates to generate 10 imputed datasets using SPSS 25.0 (Chicago, IL).²⁹ The Cox regression analyses were performed on the imputed datasets and the pooled results were presented. We used SAS 9.4 (SAS Institute, Cary, NC) and SPSS 25.0 (Chicago, IL) to perform the statistical analyses.

WMH Volumes and Clinical Outcomes

To assess whether WMH volumes were associated with clinical outcomes, we separately entered total, periventricular or confluent, and deep WMH volumes in a Cox regression model with age, sex, and intracranial volume as covariates and all-cause death, vascular-related death, nonvascular-related death, and ischemic stroke as outcomes. WMH volumes were natural log-transformed due to a non-normal distribution. In a second model, we in addition adjusted for large infarcts, lacunes, diastolic blood pressure, systolic blood pressure, diabetes mellitus, body mass index, and smoking pack-years at baseline. We also assessed the association between quartiles of

WMH volumes (not natural log-transformed) and clinical outcomes, adjusted for all of the aforementioned covariates.

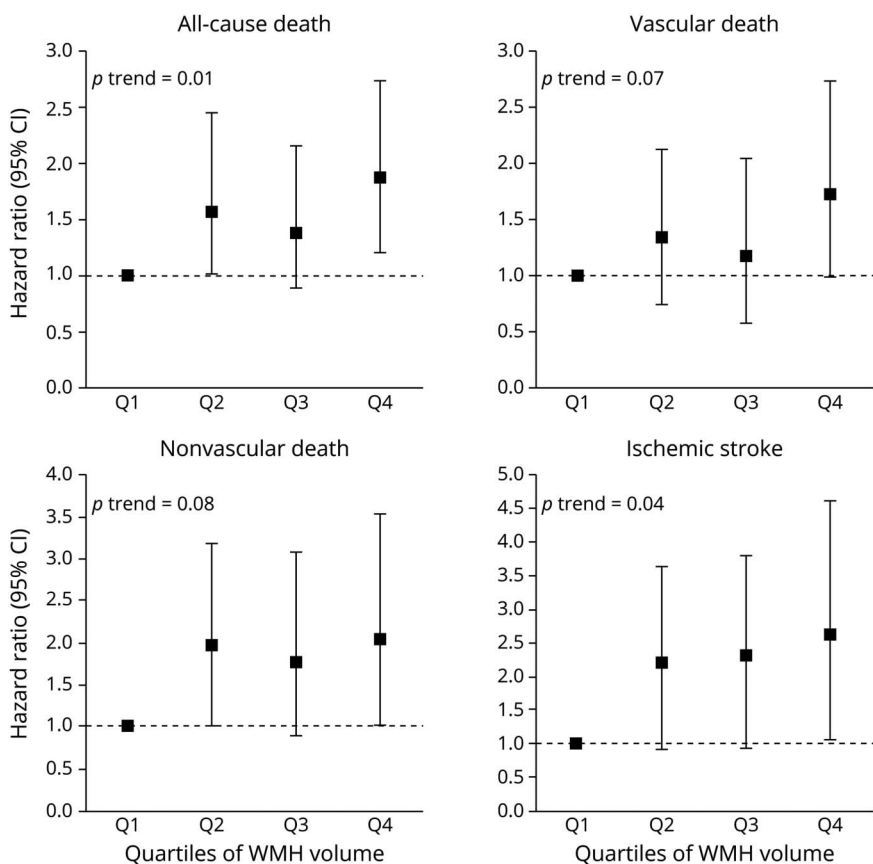
WMH Types and Clinical Outcomes

To assess whether WMH types were associated with clinical outcomes, a categorical variable with the 3 WMH types as outcomes was entered in a Cox regression model with age and sex as covariates and all-cause death, vascular-related death, nonvascular-related death, and ischemic stroke as outcomes. A periventricular WMH type without deep WMH was chosen as the reference category as this type represents the smallest WMH burden. In a second model, we in addition adjusted for the aforementioned covariates.

WMH Shape Markers and Clinical Outcomes

Z scores of WMH shape markers were calculated to facilitate comparison and these were entered in a Cox regression model with age and sex as covariates and all-cause death, vascular-related death, nonvascular-related death, and ischemic stroke as outcomes. In a second model, we in addition adjusted for the aforementioned covariates. If an association between a WMH shape marker and clinical outcome was observed, we in addition adjusted for total WMH volume to assess whether the association was independent of WMH volume.

Figure 3 Risk of Mortality and Ischemic Stroke in Relation to Quartiles of Deep White Matter Hyperintensity (WMH) Volume at Baseline



Associations between quartiles of deep WMH volume and risk of all-cause death, vascular death, nonvascular death, and ischemic stroke. Results adjusted for age, sex, intracranial volume, large infarcts on MRI, lacunes on MRI, diastolic blood pressure, systolic blood pressure, diabetes mellitus, body mass index, and smoking pack-years at baseline. The lowest quartile (<0.03 mL) was chosen as the reference category. Range second to fourth quartiles; 0.03–0.08 mL, 0.08–0.35 mL, \geq 0.35 mL, respectively. Note that the scale of the y-axis may differ between outcomes. CI = confidence interval.

Data Availability

For use of anonymized data, a reasonable request has to be made in writing to the study group and the third party has to sign a confidentiality agreement.

Results

Baseline characteristics of the study sample ($n = 999$) are shown in table 1. A total of 784 patients (78%) had periventricular WMH and 215 patients (22%) had confluent WMH. A periventricular with deep WMH type was present in 423 patients (42%) and a periventricular without deep WMH type was present in 361 patients (36%). In total, 274 patients died (149 vascular-related and 125 nonvascular-related) and 75 patients had an ischemic stroke during a median follow-up of 12.5 years (range 0.2–16.0 years; total number of person-years follow-up 11,303).

Associations Between WMH Volumes and Long-term Clinical Outcomes

Greater total WMH volume was associated with all-cause death (HR 1.32, 95% confidence interval [CI] 1.19–1.46 for a 1-unit increase in natural log-transformed total WMH

volume), particularly vascular-related death (HR 1.29, 95% CI 1.29–1.68) and to a lesser extent nonvascular-related death (HR 1.15, 95% CI 0.99–1.34), as well as with ischemic stroke (HR 1.79, 95% CI 1.48–2.16), adjusted for age, sex, and total intracranial volume. These associations persisted after adjusting for cardiovascular risk factors and cerebrovascular disease (table 2).

Greater periventricular or confluent WMH volume was associated with all-cause death (HR 1.29, 95% CI 1.17–1.42), particularly vascular-related death (HR 1.43, 95% CI 1.26–1.63), and to a lesser extent with nonvascular-related death (HR 1.14, 95% CI 0.99–1.32), as well as with ischemic stroke (HR 1.73, 95% CI 1.45–2.08). These associations persisted after adjusting for cardiovascular risk factors and cerebrovascular disease (table 2).

Greater deep WMH volume was associated with all-cause death (HR 1.13, 95% CI 1.04–1.24), vascular-related death (HR 1.15, 95% CI 1.03–1.30), and more strongly with ischemic stroke (HR 1.24, 95% CI 1.05–1.46). Risk estimates slightly attenuated after adjusting for cardiovascular risk factors and cerebrovascular disease (table 2). A nonsignificant association was observed between greater deep WMH volume

Table 3 Results of Cox Proportional Hazard Regression Analyses With White Matter Hyperintensity (WMH) Types as Independent Variables and All-Cause, Vascular-Related, and Nonvascular-Related Death and Ischemic Stroke as Dependent Variables

	Deaths or events, n	N per 1,000 person-years	Model 1, estimate (95% CI)	Model 2, estimate (95% CI)
Periventricular without deep WMH (n = 360)				
All-cause death	60	13.7	1 (reference)	1 (reference)
Vascular death	27	6.2	1 (reference)	1 (reference)
Nonvascular death	33	7.5	1 (reference)	1 (reference)
Ischemic stroke	13	3.0	1 (reference)	1 (reference)
Periventricular with deep WMH (n = 424)				
All-cause death	105	21.5	1.27 (0.92–1.75)	1.14 (0.82–1.58)
Vascular death	58	11.9	1.53 (0.96–2.42)	1.31 (0.82–2.09)
Nonvascular death	47	9.6	1.06 (0.68–1.67)	1.01 (0.64–1.59)
Ischemic stroke	28	5.9	1.75 (0.90–3.41)	1.48 (0.75–2.91)
Confluent WMH (n = 215)				
All-cause death	109	53.3	2.29 (1.64–3.19)	1.74 (1.23–2.47)
Vascular death	64	31.3	2.81 (1.75–4.49)	1.89 (1.15–3.11)
Nonvascular death	45	22.0	1.85 (1.15–2.98)	1.65 (1.01–2.73)
Ischemic stroke	34	17.8	4.36 (2.20–8.65)	2.83 (1.36–5.87)

Abbreviation: CI = confidence interval.

Estimates represent hazard ratios (95% CI) for WMH types. A periventricular WMH type without deep WMH was the reference category. Model 1: adjusted for age and sex. Model 2: model 1 in addition adjusted for large infarcts on MRI, lacunes on MRI, diastolic blood pressure, systolic blood pressure, diabetes mellitus, body mass index, and smoking pack-years at baseline.

and nonvascular death (HR 1.10, 95% CI 0.96–1.26), which did not change after adjusting for cardiovascular risk factors and cerebrovascular disease (table 2).

Risk of vascular-related death and ischemic stroke increased per quartile of periventricular or confluent WMH volume (figure 2). Similarly, risk of ischemic stroke increased per quartile of deep WMH volume (figure 3).

Associations Between WMH Types and Long-term Clinical Outcomes

Compared to a periventricular WMH type without deep WMH, a confluent WMH type was associated with a greater risk of all-cause death (HR 2.29, 95% CI 1.64–3.19), particularly vascular-related death (HR 2.81, 95% CI 1.75–4.49) and to a lesser extent nonvascular-related death (HR 1.85, 95% CI 1.15–2.98), as well as with ischemic stroke (HR 4.36, 95% CI 2.20–8.65). These associations persisted after adjusting for cardiovascular risk factors and cerebrovascular disease (table 3). Nonsignificant associations were observed between a periventricular WMH type with deep WMH and vascular-related death (HR 1.53, 95% CI 0.96–2.42) and ischemic stroke (HR 1.75, 95% CI 0.90–3.41), which attenuated after adjusting for cardiovascular risk factors and cerebrovascular disease (table 3).

Associations Between WMH Shape Markers and Long-term Clinical Outcomes

A greater concavity index of periventricular or confluent WMH was associated with a greater risk of all-cause death (HR 1.30, 95% CI 1.18–1.43 per SD increase), particularly vascular-related death (HR 1.34, 95% CI 1.18–1.52) and to a lesser extent nonvascular-related death (HR 1.25, 95% CI 1.07–1.45), as well as with ischemic stroke (HR 1.47, 95% CI 1.23–1.76), adjusted for age and sex. These associations persisted after adjusting for cardiovascular risk factors and cerebrovascular disease (table 4). After in addition adjusting for total WMH volume, the association of concavity index with all-cause and nonvascular-related death persisted (HR 1.21, 95% CI 1.02–1.42; HR 1.23, 95% CI 1.02–1.49, respectively), whereas the association with vascular-related death and ischemic stroke attenuated (HR 1.11, 95% CI 0.89–1.39; HR 1.23, 95% CI 0.95–1.77, respectively).

A greater fractal dimension of periventricular or confluent WMH was associated with a greater risk of all-cause death (HR 1.33, 95% CI 1.16–1.52 per SD increase), vascular-related death (HR 1.52, 95% CI 1.27–1.82), and ischemic stroke (HR 2.06, 95% CI 1.60–2.65), adjusted for age and sex. These relationships persisted after adjusting for cardiovascular risk factors and cerebrovascular disease (table 4). After in

Table 4 Results of Cox Proportional Hazard Regression Analyses With Standardized White Matter Hyperintensity (WMH) Shape Markers as Independent Variables and All-Cause, Vascular-Related, and Nonvascular-Related Death and Ischemic Stroke as Dependent Variables

	Deaths or events, n	N per 1,000 person-years	Model 1, estimate (95% CI)	Model 2, estimate (95% CI)
Periventricular or confluent WMH				
Concavity index				
All-cause death	274	24.2	1.30 (1.18–1.43)	1.21 (1.09–1.35)
Vascular death	149	13.2	1.34 (1.18–1.52)	1.20 (1.05–1.38)
Nonvascular death	125	11.1	1.25 (1.07–1.45)	1.21 (1.03–1.42)
Ischemic stroke	75	6.8	1.47 (1.23–1.76)	1.28 (1.05–1.55)
Fractal dimension				
All-cause death	274	24.2	1.33 (1.16–1.52)	1.19 (1.04–1.36)
Vascular death	149	13.2	1.52 (1.27–1.82)	1.29 (1.08–1.55)
Nonvascular death	125	11.1	1.13 (0.92–1.37)	1.06 (0.87–1.30)
Ischemic stroke	75	6.8	2.06 (1.60–2.65)	1.73 (1.33–2.25)
Deep WMH				
Fractal dimension				
All-cause death	212	30.8	1.03 (0.89–1.20)	1.07 (0.92–1.26)
Vascular death	122	17.8	1.06 (0.87–1.29)	1.11 (0.91–1.37)
Nonvascular death	90	13.1	1.00 (0.79–1.25)	1.02 (0.81–1.29)
Ischemic stroke	62	9.4	0.82 (0.63–1.06)	0.85 (0.65–1.12)
Eccentricity				
All-cause death	212	30.8	0.93 (0.81–1.07)	0.98 (0.85–1.14)
Vascular death	122	17.8	1.01 (0.84–1.21)	1.09 (0.90–1.33)
Nonvascular death	90	13.1	0.84 (0.68–1.04)	0.85 (0.68–1.07)
Ischemic stroke	62	9.4	0.99 (0.77–1.28)	1.14 (0.87–1.49)

Abbreviation: CI = confidence interval.

Estimates represent hazard ratios (95% CI) for 1 SD increase in the marker. Model 1: adjusted for age and sex. Model 2: model 1 in addition adjusted for large infarcts on MRI, lacunes on MRI, diastolic blood pressure, systolic blood pressure, diabetes mellitus, body mass index, and smoking pack-years at baseline.

addition adjusting for total WMH volume, the association of fractal dimension with all-cause death, vascular-related death, and ischemic stroke attenuated (HR 1.10, 95% CI 0.93–1.30; HR 1.20, 95% CI 0.95–1.51; HR 1.09, 95% CI 0.52–2.27, respectively). A greater fractal dimension of periventricular or confluent WMH was not associated with a greater risk of nonvascular-related death (HR 1.13, 95% CI 0.92–1.37).

No associations were observed between eccentricity and fractal dimension of deep WMH and long-term clinical outcomes (table 4).

Discussion

In this cohort of patients with manifest arterial disease, we observed that WMH volume, type, and shape were associated

with long-term clinical outcomes. Specifically, we found that a greater volume and a more irregular shape of periventricular or confluent WMH were related to a higher risk of death and ischemic stroke. A confluent WMH type was also associated with a greater risk of death and ischemic stroke. These relationships were independent of demographics, cardiovascular risk factors, and cerebrovascular disease at baseline.

Our finding that total WMH volume was related to risk of mortality and stroke is in line with previous studies.³⁰⁻³⁴ However, the associations of WMH volume subclassifications and WMH types with clinical outcomes presented in this study are novel. We found that the risk of mortality and ischemic stroke was predominantly determined by the volume of periventricular or confluent WMH, rather than the volume of deep WMH. This was supported by the observation that risk estimates for mortality and ischemic stroke were higher

for a confluent WMH type than a periventricular WMH type with deep WMH. A possible explanation for this finding may be that confluent WMH represent more severe parenchymal changes due to their relatively central location in the brain. Previous studies showed that pathologic changes in the smaller vessels of the brain can induce secondary ischemia, which may be more profound in the white matter surrounding the lateral ventricles as these regions are furthest removed from collateral circulation.^{4,35} This notion may explain the relatively strong association between a confluent WMH type and occurrence of ischemic stroke in the present study.

To our knowledge, no previous studies reported on the longitudinal association of WMH shape with clinical outcomes. In the present study, we observed that a more irregular shape of periventricular or confluent WMH was related to an increased risk of mortality and ischemic stroke, which was only partly explained by WMH volume. An explanation for this finding may be that CSVD consists of a heterogeneous group of small vessel changes and a more irregular shape of WMH may indicate the presence of a more severe CSVD subtype.^{35,36} Support for this notion is provided by histopathologic studies that reported ischemic damage, loss of myelin, and incomplete parenchymal destruction in more irregular shaped WMH, whereas smooth WMH correlated with more benign pathologic changes such as venous congestion.^{6,8,13} Furthermore, a previous study reported an association between a more irregular shape of WMH and frailty in elderly patients¹⁶ and in previous work we showed that presence of lacunes on MRI was related to a more irregular shape of WMH.¹⁴ These investigations and the results of the present study suggest that in addition to WMH volume, shape of WMH may represent a clinically relevant marker in patients with WMH on MRI.

We observed that a confluent WMH type and a more irregular shape of periventricular or confluent WMH were not only associated with a greater risk of vascular death, but also of nonvascular death. In previous work, we similarly reported that presence of lacunes on MRI was related to a greater risk of nonvascular death.³⁷ An explanation for these findings is that CSVD may be a marker of overall increased vulnerability to adverse outcomes, possibly through the concomitant presence of generalized microvascular disease.^{2,4,35} Further studies in different cohorts are needed to confirm this hypothesis, but the reported associations with vascular and nonvascular death suggest that WMH markers may be important in determining overall prognosis of patients with manifest arterial disease.

Key strengths of the present study are the large number of patients included, the longitudinal design, the relatively long follow-up period, and the use of automated image processing techniques that enabled us to examine multiple and also novel features of WMH in relation to clinical outcomes. Furthermore, all MRI scans were visually checked and corrected if needed to ensure that WMH segmentation and subsequent analysis of WMH type and shape were accurate.

Limitations of this study include, first, the use of 1.5T MRI instead of 3.0T MRI, which is likely more sensitive in detecting small WMH lesions. Clinical 3.0T MRI scanners were not readily available during the inclusion period of our study, starting in 2001. Second, we did not categorize deep WMH into lesions located directly under the cerebral cortex (i.e., infracortical) and those located more centrally in the subcortical white matter, which may differ in terms of etiology.³⁸ Third, MRI sequences were used with a relatively large slice thickness of 4 mm, which is likely less accurate in determining WMH shape markers than 3D MRI sequences. The impact of slice thickness, however, may be less profound on measurements of the concavity index as it is calculated by determining volume and surface area ratios of periventricular or confluent WMH, which are expected to remain relatively constant.¹⁴ On the other hand, a more profound impact can be expected on measurements of the fractal dimension, which is directly dependent on voxel size.¹⁴ A larger slice thickness will therefore lead to reduced information in the z-axis. Similarly, shape determination of smaller deep WMH in the size range of several millimeters may also be affected by a relatively large slice thickness. Despite this limitation, however, we were able to detect associations between WMH shape markers and clinical outcomes, suggesting that WMH shape may represent a clinically relevant marker for occurrence of ischemic stroke and death.

Our findings demonstrate that WMH volume, type, and shape are associated with long-term risk of mortality and ischemic stroke in patients with manifest arterial disease. These findings suggest that WMH markers on MRI may be useful in determining patient prognosis and may aid in future patient selection for preventive treatment.

Acknowledgment

The authors thank the research nurses, R. van Petersen (data manager), and B. van Dinther (study manager).

Study Funding

Funding for this article was received as part of a grant from the Netherlands Organization for Scientific Research—Medical Sciences (NWO-MW: project 904-65-095). This funding source had no role in the design, data collection, data analyses, or data interpretation of the study or writing of the report. Funding also was received from the European Research Council under the European Union's Horizon 2020 Programme (H2020)/ERC grant agreements 637024 and 66681 (SVDs@target).

Disclosure

The authors report no disclosures. Go to [Neurology.org/N](https://www.neurology.org/N) for full disclosures.

Publication History

Received by *Neurology* July 5, 2020. Accepted in final form January 28, 2021.

Appendix 1 Authors

Name	Location	Contribution
Rashid Ghaznawi, MD, MSc	Julius Center for Health Sciences and Primary Care, Department of Radiology, University Medical Center Utrecht and Utrecht University, the Netherlands	Literature search, figures, data collection, MRI processing, data analysis, data interpretation and writing
Mirjam I. Geerlings, PhD	Julius Center for Health Sciences and Primary Care, University Medical Center Utrecht and Utrecht University, the Netherlands	Study design, data analysis and interpretation, critically reviewed the manuscript
Myriam Jaarsma-Coes, MSc	Department of Radiology, Leiden University Medical Center, the Netherlands	MRI processing, data analysis, data interpretation, critically reviewed the manuscript
Jeroen Hendrikse, MD, PhD	Department of Radiology, University Medical Center Utrecht and Utrecht University, the Netherlands	Critically reviewed the manuscript
Jeroen de Bresser, MD, PhD	Department of Radiology, Leiden University Medical Center, the Netherlands	Study design, data interpretation, critically reviewed the manuscript

Appendix 2 The Utrecht Cardiovascular Cohort-Second Manifestations of Arterial Disease Study Group

Name	Location	Role	Contribution
F.L.J. Visseren, MD, PhD	University Medical Center Utrecht, Utrecht University, the Netherlands	Chairman; co-investigator; SMART study contributor	Critical review, responsible for data integrity, responsible for endpoint adjudication
F.W. Asselbergs, MD, PhD	University Medical Center Utrecht, Utrecht University, the Netherlands	Co-investigator; SMART study contributor	Critical review, responsible for data integrity, responsible for endpoint adjudication
H.M. Nathoe, MD, PhD	University Medical Center Utrecht, Utrecht University, the Netherlands	Co-investigator; SMART study contributor	Critical review, responsible for data integrity, responsible for endpoint adjudication
M.L. Bots, MD, PhD	Julius Center for Health Sciences and Primary Care, University Medical Center Utrecht and Utrecht University, the Netherlands	Co-investigator; SMART study contributor	Critical review, responsible for data integrity, responsible for endpoint adjudication
M.H. Emmelot, MD, PhD	University Medical Center Utrecht, Utrecht University, the Netherlands	Co-investigator; SMART study contributor	Critical review, responsible for data integrity, responsible for endpoint adjudication
G.J. de Borst, MD, PhD	University Medical Center Utrecht, Utrecht University, the Netherlands	Co-investigator; SMART study contributor	Critical review, responsible for data integrity, responsible for endpoint adjudication

Appendix 2 (continued)

Name	Location	Role	Contribution
L.J. Kappelle, MD, PhD	University Medical Center Utrecht, Utrecht University, the Netherlands	Co-investigator; SMART study contributor	Critical review, responsible for data integrity, responsible for endpoint adjudication
T. Leiner, MD, PhD	University Medical Center Utrecht, Utrecht University, the Netherlands	Co-investigator; SMART study contributor	Responsible for data integrity, responsible for endpoint adjudication
P.A. de Jong, MD, PhD	University Medical Center Utrecht, Utrecht University, the Netherlands	Co-investigator; SMART study contributor	Critical review, responsible for data integrity, responsible for endpoint adjudication
A.T. Lely, MD, PhD	University Medical Center Utrecht, Utrecht University, the Netherlands	Co-investigator; SMART study contributor	Critical review, responsible for data integrity, responsible for endpoint adjudication
N.P. van der Kaaij, MD, PhD	University Medical Center Utrecht, Utrecht University, the Netherlands	Co-investigator; SMART study contributor	Critical review, responsible for data integrity, responsible for endpoint adjudication
Y. Ruigrok, MD, PhD	University Medical Center Utrecht, Utrecht University, the Netherlands	Co-investigator; SMART study contributor	Critical review, responsible for data integrity, responsible for endpoint adjudication
M.C. Verhaar, MD, PhD	University Medical Center Utrecht, Utrecht University, the Netherlands	Co-investigator; SMART study contributor	Critical review, responsible for data integrity, responsible for endpoint adjudication
J. Westerink, MD, PhD	University Medical Center Utrecht, Utrecht University, the Netherlands	Co-investigator; SMART study contributor	Critical review, responsible for data integrity, responsible for endpoint adjudication

References

1. DeBette S, Markus HS. The clinical importance of white matter hyperintensities on brain magnetic resonance imaging: systematic review and meta-analysis. *BMJ* 2010;341:c3666.
2. Wardlaw JM, Smith C, Dichgans M. Mechanisms of sporadic cerebral small vessel disease: insights from neuroimaging. *Lancet Neurol* 2013;12:483–497.
3. Prins ND, Scheltens P. White matter hyperintensities, cognitive impairment and dementia: an update. *Nat Rev Neurol* 2015;11:157–165.
4. Wardlaw JM, Smith EE, Biessels GJ, et al. Neuroimaging standards for research into small vessel disease and its contribution to ageing and neurodegeneration. *Lancet Neurol* 2013;12:822–838.
5. Ostergaard L, Engedal TS, Moreton F, et al. Cerebral small vessel disease: capillary pathways to stroke and cognitive decline. *J Cereb Blood Flow Metab* 2016;36:302–325.
6. Gouw AA, Seewann A, van der Flier WM, et al. Heterogeneity of small vessel disease: a systematic review of MRI and histopathology correlations. *J Neurol Neurosurg Psychiatry* 2011;82:126–135.
7. Fazekas F, Kleinert R, Offenbacher H, et al. The morphologic correlate of incidental punctate white matter hyperintensities on MR images. *AJNR Am J Neuroradiol* 1991; 12:915–921.
8. Fazekas F, Kleinert R, Offenbacher H, et al. Pathologic correlates of incidental MRI white matter signal hyperintensities. *Neurology* 1993;43:1683–1689.
9. Schmidt R, Fazekas F, Kleinert G, et al. Magnetic resonance imaging signal hyperintensities in the deep and subcortical white matter. A comparative study between stroke patients and normal volunteers. *Arch Neurol* 1992;49:825–827.

10. Gouw AA, van der Flier WM, Fazekas F, et al. Progression of white matter hyperintensities and incidence of new lacunes over a 3-year period: the Leukoaraiosis and Disability Study. *Stroke* 2008;39:1414–1420.
11. van Dijk EJ, Prins ND, Vrooman HA, et al. Progression of cerebral small vessel disease in relation to risk factors and cognitive consequences: Rotterdam Scan Study. *Stroke* 2008;39:2712–2719.
12. Kloppenborg RP, Nederkoorn PJ, Grool AM, et al. Cerebral small-vessel disease and progression of brain atrophy: the SMART-MR study. *Neurology* 2012;79:2029–2036.
13. Kim KW, MacFall JR, Payne ME. Classification of white matter lesions on magnetic resonance imaging in elderly persons. *Biol Psychiatry* 2008;64:273–280.
14. Ghaznawi R, Geerlings MI, Jaarsma-Coes MG, et al. The association between lacunes and white matter hyperintensity features on MRI: the SMART-MR study. *J Cereb Blood Flow Metab* 2019;39:2486–2496.
15. de Bresser J, Kuijff HJ, Zaanen K, et al. White matter hyperintensity shape and location feature analysis on brain MRI; proof of principle study in patients with diabetes. *Sci Rep* 2018;8:1893.
16. Kant IMJ, Mutsaerts H, van Montfort SJJ, et al. The association between frailty and MRI features of cerebral small vessel disease. *Sci Rep* 2019;9:11343.
17. Geerlings MI, Appelman AP, Vincken KL, et al. Brain volumes and cerebrovascular lesions on MRI in patients with atherosclerotic disease: the SMART-MR study. *Atherosclerosis* 2010;210:130–136.
18. Goessens BM, Visseren FL, Kappelle LJ, et al. Asymptomatic carotid artery stenosis and the risk of new vascular events in patients with manifest arterial disease: the SMART study. *Stroke* 2007;38:1470–1475.
19. Ghaznawi R, Zwartbol MH, Zuithoff NP, et al. Reduced parenchymal cerebral blood flow is associated with greater progression of brain atrophy: the SMART-MR study. *J Cereb Blood Flow Metab* 2020;271678x20948614.
20. Anbeek P, Vincken KL, van Bochove GS, et al. Probabilistic segmentation of brain tissue in MR imaging. *Neuroimage* 2005;27:795–804.
21. Kempton MJ, Underwood TS, Brunton S, et al. A comprehensive testing protocol for MRI neuroanatomical segmentation techniques: evaluation of a novel lateral ventricle segmentation method. *Neuroimage* 2011;58:1051–1059.
22. Fazekas F, Chawluk JB, Alavi A, et al. MR signal abnormalities at 1.5 T in Alzheimer's dementia and normal aging. *AJR Am J Roentgenol* 1987;149:351–356.
23. Fazekas F, Barkhof F, Wahlund LO, et al. CT and MRI rating of white matter lesions. *Cerebrovasc Dis* 2002;13(suppl 2):31–36.
24. Liu EJ, Cashman KV, Rust AC. Optimising shape analysis to quantify volcanic ash morphology. *GeoResJ* 2015;8:14–30.
25. Zhang L, Liu JZ, Dean D, et al. A three-dimensional fractal analysis method for quantifying white matter structure in human brain. *J Neurosci Methods* 2006;150:242–253.
26. Esteban FJ, Sepulcre J, de Miras JR, et al. Fractal dimension analysis of grey matter in multiple sclerosis. *J Neurol Sci* 2009;282:67–71.
27. Loizou CP, Petroudi S, Seimenis I, et al. Quantitative texture analysis of brain white matter lesions derived from T2-weighted MR images in MS patients with clinically isolated syndrome. *J Neuroradiol* 2015;42:99–114.
28. Murphy K, van Ginneken B, Schilham AM, et al. A large-scale evaluation of automatic pulmonary nodule detection in chest CT using local image features and k-nearest-neighbour classification. *Med Image Anal* 2009;13:757–770.
29. White IR, Royston P, Wood AM. Multiple imputation using chained equations: issues and guidance for practice. *Stat Med* 2011;30:377–399.
30. Weinstein G, Wolf PA, Beiser AS, et al. Risk estimations, risk factors, and genetic variants associated with Alzheimer's disease in selected publications from the Framingham Heart Study. *J Alzheimers Dis* 2013;33(suppl 1):S439–S445.
31. Lim JS, Hong KS, Kim GM, et al. Cerebral microbleeds and early recurrent stroke after transient ischemic attack: results from the Korean Transient Ischemic Attack Expression Registry. *JAMA Neurol* 2015;72:301–308.
32. Kuller LH, Arnold AM, Longstreth WT Jr, et al. White matter grade and ventricular volume on brain MRI as markers of longevity in the Cardiovascular Health Study. *Neurobiol Aging* 2007;28:1307–1315.
33. Henneman WJ, Sluimer JD, Cordonnier C, et al. MRI biomarkers of vascular damage and atrophy predicting mortality in a memory clinic population. *Stroke* 2009;40:492–498.
34. DeBette S, Beiser A, DeCarli C, et al. Association of MRI markers of vascular brain injury with incident stroke, mild cognitive impairment, dementia, and mortality: the Framingham Offspring Study. *Stroke* 2010;41:600–606.
35. Pantoni L. Cerebral small vessel disease: from pathogenesis and clinical characteristics to therapeutic challenges. *Lancet Neurol* 2010;9:689–701.
36. Rost NS, Rahman RM, Biffi A, et al. White matter hyperintensity volume is increased in small vessel stroke subtypes. *Neurology* 2010;75:1670–1677.
37. Conijn MM, Kloppenborg RP, Algra A, et al. Cerebral small vessel disease and risk of death, ischemic stroke, and cardiac complications in patients with atherosclerotic disease: the Second Manifestations of Arterial Disease-Magnetic Resonance (SMART-MR) study. *Stroke* 2011;42:3105–3109.
38. Wiggins ME, Jones J, Tanner JJ, et al. Pilot investigation: older adults with atrial fibrillation demonstrate greater brain leukoaraiosis in infracortical and deep regions relative to non-atrial fibrillation peers. *Front Aging Neurosci* 2020;12:271.